Precision Agric (2013) 14:541–557
DOI 10.1007/s11119-013-9315-8

Retrieval of biophysical vegetation parameters using simultaneous inversion of high resolution remote sensing imagery constrained by a vegetation index

A. J. Berjón · V. E. Cachorro · P. J. Zarco-Tejada · A. de Frutos

Published online: 5 May 2013

Abstract This study proposes a new method for inverting radiative transfer models to retrieve canopy biophysical parameters using remote sensing imagery. The inversion procedure is improved with respect to standard inversion, and achieves simultaneous inversion of leaf area index (LAI), soil reflectance (ρ_{soil}), chlorophyll content (C_{a+b}) and average leaf angle (ALA). In this approach, LAI is used to constrain modelling conditions during the inversion process, providing information about the phenological state of each plot under study. Due to the small area of the vegetation plots used for the inversion procedure and in order to avoid redundant information and improve computation efficiency, existing plot segmentation was used. All retrieved biophysical parameters, except LAI, were assumed to be invariant within each plot. The proposed methodology, based on the combination of PROSPECT and SAILH models, was tested over 16 cereal fields and 51 plots, on two dates, which were chosen to ensure crop assessment at different phenological stages. Plots were selected to provide a wide range of LAI between 0 and 6. Field measurements of LAI, ALA and C_{a+b} were conducted and used as ground truth for validation of the proposed model-inversion methodology. The approach was applied to very high spatial resolution remote sensing data from the QuickBird 2 satellite. The inversion procedure was successfully applied to the imagery and retrieved LAI with $R^2 = 0.83$ and RMSE = 0.63 when compared to LAI2000 ground measurements. Separate inversions for

A. J. Berjón · V. E. Cachorro (✉) · A. de Frutos
Grupo de Optica Atmosférica (GOA-UVA), Universidad de Valladolid, Valladolid, Spain
e-mail: chiqui@goa.uva.es

Present Address:
A. J. Berjón
Atmospheric Research Center (CIAI-AEMET), Spanish Meteorological Service, Santa Cruz de Tenerife, Spain

P. J. Zarco-Tejada
Instituto de Agricultura Sostenible (IAS), Consejo Superior de Investigaciones Científicas (CSIC), Córdoba, Spain

P. J. Zarco-Tejada
MARS-GeoCAP, Institute for Environment and Sustainability (IES), Joint Research Centre (JRC), European Commission, Ispra, Italy

barley and wheat yielded $R^2 = 0.89$ (RMSE = 0.64) and $R^2 = 0.56$ (RMSE = 0.61), respectively.

Keywords Radiative transfer model inversion · Leaf area index (LAI)

Introduction

Satellite sensors are probably the most cost-effective way to survey large areas of vegetation and to obtain useful information for application in agriculture, environment, ecology and atmospheric sciences (Liang 2004, 2008; Fernández et al. 2010; King et al. 1999; Kaufman et al. 2002). Remote sensing applied to agricultural monitoring requires the conversion of spectral data to quantifiable agricultural output data. Vegetation properties that can be derived from remote sensing data analysis are those that play an active role in the interaction process between radiation and vegetation. There are two main groups of properties: structural properties such as leaf area and leaf inclination angle; and optical properties of certain vegetation components such as water or dry matter and pigments such as chlorophyll or carotenoids.

Leaf area index (LAI) is one of the most important structural parameters for crop monitoring. It is defined as the one-sided leaf area per unit of ground surface area and is related to crop productivity, evapotranspiration and surface energy balance. Currently, the most widely extended method to estimate LAI from remote sensing images is the use of vegetation indices such as NDVI (Haboudane et al. 2002). Several studies have related NDVI to LAI (Turner et al. 1999; Zarco-Tejada et al. 2004); nonetheless, accurate retrieval of LAI from NDVI requires ground truth data for calibration (Green et al. 2000). Other techniques are also needed to improve the correlation between NDVI and LAI, e.g. angular correction for different vegetation types and different seasons, to account for differences in canopy structure (Gutman 1991). However, although vegetation indices from different satellite sensors are well correlated, the relationships are not one-to-one (Steven et al. 2003).

Over the past 10 years, radiative transfer simulation, by means of leaf and canopy modelling, has become an alternative for use in vegetation parameter retrievals. However, the retrieval of biophysical variables using canopy reflectance models can be hampered by the fact that the inverse problem is ill-posed (Combal et al. 2002) and initially lacks computational efficiency (Jacquemoud et al. 1995). Although the latter issue has been partially solved by the arrival of powerful computers in the last decade, this remains a major drawback.

Some studies assessing remote sensing LAI products (Morisette et al. 2006; Jacquemoud et al. 2009; Migdall et al. 2009) concluded that more efforts are needed to improve the accuracy of LAI retrievals. New strategies have emerged in recent years, in attempts to solve the problems that are inherent to these methodologies, particularly when several biophysical parameters are to be retrieved simultaneously. One of the proposals to resolve the ill-posed inverse problem was to add new constraints and to analyse spatial and temporal series separately or in combination, and/or use prior knowledge (Atzberger 2004). Similarly, different strategies are used depending on the type of sensor: satellite-based (Houborg et al. 2007); airborne (Migdall et al. 2009); or in situ measurements such as field spectroradiometers (Darvishzadeh et al. 2008).

The aim of the work was to explore a different approximation procedure. Specifically, spatially distributed data were assessed, bearing in mind that many of the vegetation

properties within an area such as a plot remain invariant. The proposed method was based on the assumption that the inversion procedure could be improved by simultaneously analyzing a cluster of canopy spectra, duly constraining the parameters used by the models. Vegetation indices were used to constrain input parameters, thus reducing the amount of a priori knowledge required with respect to vegetation conditions.

Materials and methods

Forward radiative transfer modelling methods

In order to estimate the biophysical properties of the vegetation in this study, two RTM models were selected and combined: the PROSPECT leaf optics model was coupled with the canopy SAILH model, thus linking leaf and canopy properties. Both models have been extensively validated and referenced (Goel 1988; Jacquemoud et al. 2009). We used version 3 of PROSPECT, which is a prior version to the modified version (version 4) that incorporated a parameter for brown pigment content that accounts for dry leaves among the vegetation. The combined model used in this study preceded the use of PROSAIL nomenclature (as per Jacquemoud et al. 2009) and thus preceded recent modifications and enhancements to the two models (Feret et al. 2008; Verhoef and Bach 2007).

The PROSPECT model (Jacquemoud and Baret 1990) simulates leaf reflectance (ρ_{leaf}) and leaf transmittance (τ_{leaf}) as a function of certain leaf components (chlorophyll as C_{a+b}, dry matter as C_m and water content as C_w) and a structural parameter. This model, which is derived from the Plate model (Allen et al. 1969), simplifies the internal structure of a leaf by considering it as a stack of a number (N) of rough plates, separated by air (Allen et al. 1970; Gausman et al. 1970). The plates are defined by a refraction index and an absorption coefficient calculated from the leaf components. In practice, N is not limited to discrete values. The SAIL model (Verhoef 1984) simulates canopy reflectance (ρ) as a function of ρ_{leaf}, τ_{leaf}, plant structure (LAI and leaf angle distribution), soil reflectance (ρ_{soil}), angles of observation (θ_o and φ_o) and sun elevation (θ_s) and likewise, the relation between global and direct illumination, SKYL. A subsequent modified version of the model was developed—SAILH—which takes the self-shading effect of the canopy into account (Kuusk 1985), including the hot spot parameter. Vegetation was considered as a homogeneous layer over a Lambertian soil surface. Directional reflectance of vegetative canopy was modelled using four fluxes following the first step described in the self-consistent field method (Suits 1972).

Inversion procedure

Iterative optimization is a traditional method (Jacquemoud et al. 1995, 2009; Zarco-Tejada et al. 2001) for inverting radiative transfer models in remote sensing. The technique consists of minimizing a function that frequently calculates the root mean square error between the measured and estimated quantities (Eq. 1) by means of successive input parameter iterations. A multi-start downhill simplex method (Nelder and Mead 1965) was used as a global minimization technique for the iterative optimization.

$$\Delta^2 = \sum_{\lambda} \left(\rho(\lambda) - \rho^*(\lambda, P)\right)^2 \quad (1)$$

In the above expression, $\rho(\lambda)$ is the measured canopy spectral reflectance, $\rho^*(\lambda, P)$ is the modelled canopy spectral reflectance and P represents the parameters used in the

model. An alternative merit function, Eq. (2), can be defined in order to avoid a stronger influence of the infrared region than visible region and thus improve sensitivity in the chlorophyll band absorption wavelengths due to the higher reflectance values in the infrared (Bacour et al. 2002). Weighting factors proportional to the inverse of the measured canopy reflectance can be used to achieve this objective.

$$\Delta^2 = \sum_{\lambda} \left(\frac{\rho(\lambda) - \rho^*(\lambda, P)}{\rho(\lambda)} \right)^2 \tag{2}$$

In this study, both functions were used for the inversion process, with considerable improvement in the results when using the second function. A simultaneous analysis of different canopy spectra can be done by modifying the merit function using an expression like Eq. (3) when the whole set of analysed data share certain similarities, as in the case of data from a single plot.

$$\Delta^2 = \sum_{i} \sum_{\lambda} \left(\frac{\rho_i(\lambda) - \rho_i(\lambda, P)}{\rho_i(\lambda)} \right)^2 \tag{3}$$

The modelled canopy spectra $\left(\rho_i^*\right)$ where i indicates each of the spectra considered can be calculated using some invariant parameters. Biophysical parameters that cannot be considered invariant will be constrained by the use of a vegetation index. In this expression, P' no longer means the model input parameters, as was the case in Eq. (1), but refers instead to parameters linked to vegetation indices such as LAI.

In this work, all unknown biophysical parameters were considered to be invariant within the same field plot, with the exception of LAI. Although this assumption may seem to be very restrictive, it has been used by other authors (Lauvernet et al. 2008) and was deemed to be realistic for the conditions of this study (small plot, i.e. spatial homogeneity). In order to reduce computation-time and avoid redundant information, a classification was made of each plot, as described below. Thus, sub-index i refers here to the number of classes for each plot. The LAI was accounted for through the Normalized Difference Vegetation Index (NDVI), Eq. (4).

$$NDVI = \frac{\rho_{IR} - \rho_R}{\rho_{IR} + \rho_R} \tag{4}$$

In order to constrain LAI through the NDVI, different analytical relationships can be applied. A linear relationship between LAI and NDVI was established for LAI of less than three (Zhangshi and Williams 1997), but not for higher values, where the LAI-NDVI relation becomes characteristically asymptotic (Carlson and Ripley 1990). Some authors have proposed exponential relations (Eq. 5) up to LAI 7 (Richardson et al. 1992; Lu et al. 2004).

$$LAI = x_1 e^{x_2 NDVI} \tag{5}$$

Others (Aparicio et al. 2000) have used a modified expression like Eq. (6).

$$LAI = x_1 e^{x_2 NDVI} + x_3 \tag{6}$$

This expression is more suitable for low LAI values, although it introduces a third parameter. Nevertheless, x_3 can be related to x_1, x_2, and soil reflectance when LAI is taken as being 0, and therefore, the use of the latter expression does not increase the number of parameters required.

Leaf inclination distribution function

The leaf inclination distribution functions (LIDF) in the SAIL model were originally defined by Bunnik (1978) and were included as tabulated values. Other authors (Bacour et al. 2002) have taken a different approach, e.g. using parametric functions to describe LIDF. In this study, the ellipsoidal function, as presented by Campbell (1986), was used as a continuous parameter for leaf inclination within the model. This function represents fewer possible distributions than other alternatives proposed in the literature (Goel and Strebel 1983; Kuusk 1995), but it is nonetheless adequate for most of the distributions to be found in nature (Jacquemoud et al. 1995). It has the advantage that it uses only one parameter, χ, known as the Campbell parameter. Equation (7) gives an analytical expression for the elliptical distribution function (Campbell 1990).

$$f_L(\alpha) = \frac{2\chi^3 \sin\alpha}{\Lambda\left(\cos^2\alpha + \chi^2 \sin^2\alpha\right)^2} \tag{7}$$

where α is the average leaf angle, which appears as the ALA parameter in the SAIL model and Λ is given by

$$\Lambda = \chi + 1.774(\chi + 1.182)^{-0.733} \tag{8}$$

The χ parameter is related to ALA, as shown in Eqs. (9) and (10) (Wang and Jarvis 1988).

$$ALA = \left\{(0.0066\chi + 0.0107)^{-1}\right\} \quad \text{if } \chi \leq 1 \tag{9}$$

$$ALA = \left\{(0.0103\chi + 0.0053)^{-1}\right\} \quad \text{if } \chi > 1 \tag{10}$$

Using these expressions, it is possible to relate the functions defined by Bunnik (1978) to the elliptical distribution output at specific values of χ, as shown in Table 1.

Quantitative sensitivity analysis

The objective of a sensitivity analysis is to determine how a given model depends on its input parameters (Saltelli et al. 1999). A quantitative sensitivity analysis may help identify the most important parameters of a model in order to correctly determine which of the variables can be estimated through model inversion. It also helps to define which parameters have little influence and can be fixed to typical values. The methodology proposed by Saltelli (2002) was used to sort the input parameters in order of importance. The criterion used is the unconditional value V (Y), where Y is the model output when all parameters vary between certain limits, except parameter X_i, which is fixed to its true value X_i*. Thus, if X_i is the most important parameter, then V (Y | $X_i = X_i$*) is minimal. The

Table 1 Relationship between χ and the classical leaf inclination distribution function through the mean leaf angle inclination parameter

Distribution	Plagiophile	Uniform	Spherical	Erectophile
X	3	1.5	1	0.5
MTA	28	47	58	74

problem is that the true value for X_i* is unknown; accordingly, the solution is to use the average value E (V (Y | X_i)). Considering that V = V (E (Y | X_i)) + E (V (Y | X_i)), then it is possible to alternatively maximize V (E (Y | X_i)), or normalize S_i = V (E (Y | X_i))/V (Y). This approach was used in this study to conduct the quantitative sensitivity analysis of the models.

The quantitative sensitivity analysis was first applied to the PROSPECT model using only basic optical parameters, i.e. the refractive index n, absorption coefficient k and structure parameter N. Parameters are shown in Table 2, in order of importance, thus the absorption coefficient is ranked first and the refraction index last. Figure 1 shows the results of the sensitivity analysis on PROSPECT standard inputs (N, C_{a+b}, C_w and C_m). The specific absorption coefficients are wavelength-dependent and therefore, the importance of each parameter depends on the spectral region. The analysis for reflectance and transmittance are very similar. The most critical parameters in the visible region are N and C_{a+b}, while N affects mostly the near infrared.

According to the sensitivity analysis applied to the SAILH model, using the ellipsoidal distribution function as described in Table 3, the most important input parameters were leaf reflectance and transmittance, ρ_{soil}, χ and LAI.

Satellite remote sensing data and atmospheric correction

To assess the applicability of the proposed inversion method to two crop growth stages, satellite images were acquired on 6 April and 17 May 2003 along with ground truth data. On the first date, plants were still small and soil reflectance played an important role in canopy reflectance. On the second date, plants had already reached maximum development and accordingly, the influence of soil reflectance was considerably reduced. The QuickBird 2 sensor provided imagery with four multispectral bands having wavelengths centred at 487, 548, 653 and 806 nm (FWHM of 70, 80, 60 and 140 nm, respectively) with a spatial resolution between 2.4 and 2.8 m. A panchromatic band was also available, covering the 445–900 nm spectral range with a spatial resolution of 60–70 cm, depending on the view angle. QuickBird 2 was in a sun-synchronous polar orbit at an altitude of 450 km, with an inclination angle of 97.2° and equatorial crossing time at 10:30 a.m. Revisit times ranged from 1 to 3.5 days, depending on the latitude.

The standard multispectral product was chosen since it is radiometrically and geometrically corrected. Radiometric corrections include conversion to absolute units of radiance, L_{sat}. The product is delivered with uniform pixel size of 2.8 m. Although the images are georeferenced, the error in coordinates may exceed 80 m (Liedtke 2002); accordingly, a second geometrical correction was made using GPS ground control points.

Table 2 Refractive index n, absorption coefficient k and structure parameter N used in PROSPECT, ranked in order of importance

Parameter	$S_i(\rho)$	$S_i(\tau)$
k	0.954	0.945
N	0.140	0.121
n	0.138	0.065

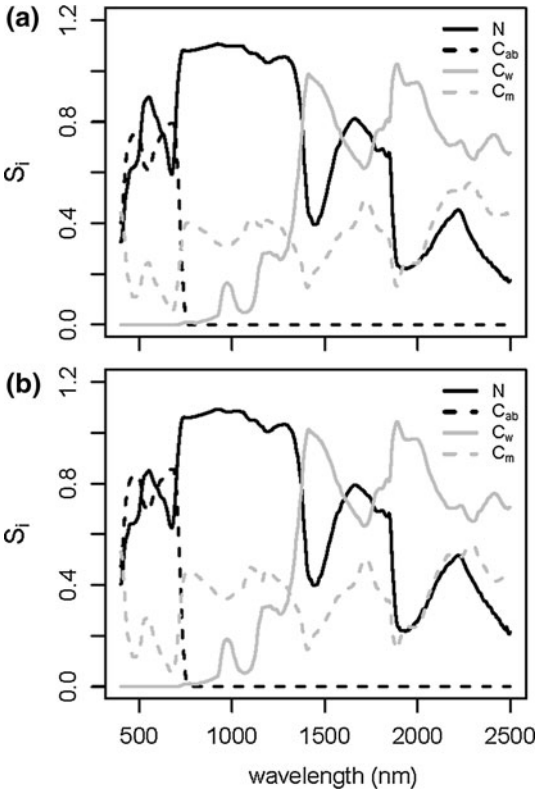

Fig. 1 PROSPECT inputs ranked in order of importance for **a** reflectance and **b** transmittance

Table 3 SAILH inputs in order of importance

Parameter	S_i
ρ_{leaf}	0.699
τ_{leaf}	0.312
ρ_{soil}	0.251
X	0.170
LAI	0.115
HotSpot	0.078
θ_o	0.036
φ_o	0.036
SKYL	0.031
θ_s	0.011

Reflectance at satellite level was calculated from radiance values for each band, according to Eq. (11) (Vermote et al. 1997), where θ_S is the solar zenith angle and E_s is the extra-terrestrial solar irradiance (using the Gueymard 2004 spectra).

$$\rho^* = \frac{\pi L_{sat}}{\cos(\theta_s) E_s} \tag{11}$$

Atmospheric correction of reflectance of the satellite images was made using 6S Code (Vermote et al. 1997) by means of the following expression:

$$\rho^*(\theta_s, \theta_o, \phi_o) = T_g(\theta_s, \theta_o)\left\{\rho_a(\theta_s, \theta_o, \phi_o) + \frac{T(\theta_s)T(\theta_o)\rho}{1 - S\langle\rho\rangle}\right\} \tag{12}$$

Where the total transmittance (T_g) of the atmosphere is explained by the selective absorption of molecular gases, considering the double pathway of sun-earth-satellite given by θ_S and θ_0; ρ_a being reflectance of the atmosphere; S, spherical albedo and T, the global scattering transmittance of the atmosphere for the solar zenith angle and the satellite view angle, respectively. These three functions were evaluated, assuming a scattering atmosphere as a mixture of aerosols and molecules, with no absorbing gases (non-absorbing atmosphere; for further details, see Cachorro et al. 1997, 2000). Aerosol optical thickness and other optical parameters required for the atmospheric correction conducted with 6S were obtained from a station located in Palencia (Spain) belonging to the AERONET network (Bennouna et al. 2013), which is located 45 km away from the study area. Columnar water vapour content was also taken from the AERONET data of this station. Columnar ozone content was obtained from the TOMS database (http://wdc.dlr.de/sensors/toms/, last view 25 March 2013). Pixel reflectance (ρ) and the reflectance of the environment of a given pixel $\langle\rho\rangle_i$ were evaluated as the mean value of the whole image.

Ground measurements

The LAI, C_{a+b} and ALA were measured from the full set of parameters required by the SAILH and PROSPECT models. Ground measurements on 16 plots were performed several days prior to and following the date planned for image acquisition. Sampling was conducted in this way because of the difficulty in determining the exact date of the image acquisition for this satellite sensor, which has a long acquisition window. Area of sample plots ranged from 0.5 to 22 ha and averaged $\sim$8 ha. Considering the QuickBird 2 spatial resolution, this would mean that between 734 and 28 718 pixels were used to characterize each plot. Coordinates of the measurement points were determined by GPS. Coordinates of auxiliary control points, which are easily distinguishable in images, were also determined to accurately locate measurement points on the images.

An LAI-2000 Plant Canopy Analyzer (Li-Cor Inc., Lincoln, NE, USA) was used to obtain measurements of the canopy structure. The principal magnitude derived from this instrument is LAI, but ALA can also be derived. Three different locations were measured with the LAI2000 to characterize each of the 16 plots. A total of 51 sites were measured on each date. Points were selected in order to have a wide gradient of LAI. Measured LAI values ranged from 0.1 to 3.3 on 6 April and from 1.4 to 6.1 on 17 May. Measured values of ALA were very similar for all control points, with an average value of 61°, corresponding to a value of 0.8 for the parameter χ with a standard deviation of 9°. Leaf chlorophyll content (C_{a+b}) was determined by destructive sampling (Zarco-Tejada et al. 2005). Ten leaves per plot were collected. A circular sample (0.7-cm dia.) from each leaf was dissolved in 12 ml acetone (80 %). Absorbance spectra were determined using a Jasco UV–VIS V-530 spectrophotometer (Easton, MD, USA) and C_{a+b} was calculated using the extinction coefficients derived by Wellburn (1994). Laboratory measured chlorophyll concentration values ranged from 6.8 to 78.8 $\mu g/cm^2$ with an average value of 34.9 $\mu g/cm^2$

and a standard deviation of 13.7 μg/cm^2. Average values of C_{a+b} across each of the 16 selected plots varied between 20 and 60 μg/cm^2 as shown in Fig. 7.

Soil background reflectance has a relatively large impact on reflectance spectra, especially in the near-infrared (NIR), being wavelength dependent. In the case of Quickbird 2 sensor, four parameters were needed to account for the spectral information. Therefore, to account for soil reflectance, the NIR, green and blue bands from the QuickBird 2 sensor were related to the red band (see Fig. 2) using a soil reflectance database (Cachorro et al. 2001). Such database comprised soil spectra collected over extended plots in the area of study at different time points over a period of 4 years. Thus, only one parameter, i.e. reflectance of the red band (ρ_{soil}) was used to estimate reflectance for the other bands. The study was repeated using spectra from the Johns Hopkins University soil reflectance database (ENVI software package). No significant differences were found in the established correlations.

The minimization procedure consisted of leaving parameters C_{a+b}, ρ_{soil} and x_1 (relating LAI and NDVI) free to vary during iterative optimization. The value of N was fixed at 1.5 (Jacquemoud and Baret 1990), and that of C_m at 0.003 g/cm^2 (Vile et al. 2005). As the observation angle was outside the hot spot region, HotSpot was set to zero. The value of C_w was also set to zero, given that water absorption is negligible at the wavelengths used. The ratio between direct and diffuse radiation—the SKYL parameter—was evaluated using the VISIBLE-NIR-GOA model (Cachorro et al. 1997, 2000). This is a simple parameterised one-layer solar radiative transfer model using experimental atmospheric data from the Cimel-AERONET photometer. Ozone atmospheric content was taken from TOMS data. The model had been previously tested for determining this parameter in a field radiometric campaign conducted in 2002 (Berjón et al. 2006).

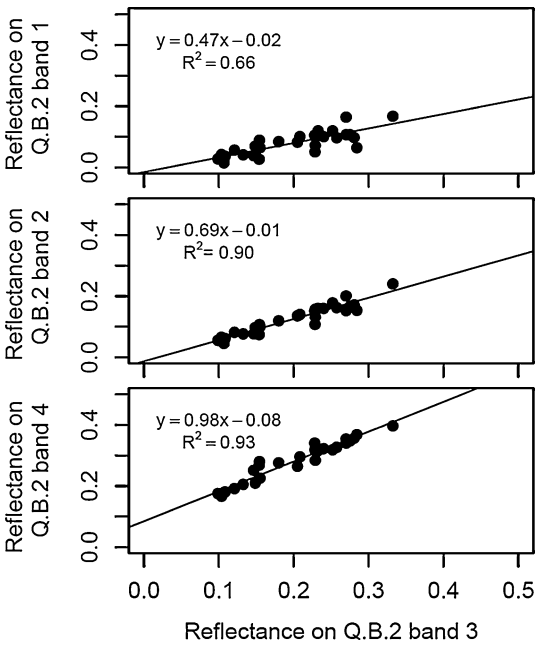

Fig. 2 Relationships obtained between QuickBird-2 bands 1, 2 and 4 with band 3 for ground-based measured soil reflectance

Results and discussion

Application of the inverse retrieval method

The size of the study areas ranged between 734 and 28 718 pixels and accordingly, simultaneous analysis of data at the pixel level required an extremely long computation time when using iterative methods. Results for the inversion applied to the mean reflectance value for each k-means clustering-derived class are reported in this section using different tests performed with 5, 10, 15, 20 and 25 classes per plot (in line with Berjón 2007). The global minimization method employed a multi-start downhill simplex method, which required restarting several times for each plot using different initial estimates (Table 4). Since the value of LAI depends on x_1, x_2 and ρ_{soil}, different initial estimates were used for x_1 and ρ_{soil}, fixing x_2 to 0.01. Figure 3 shows the NDVI obtained from reflectance and LAI retrieved by inversion for plot number 2 on 6 April using 10 classes and constraining χ between 0.7 and 0.9.

Correlations between all LAI values measured and obtained by inversion are shown in Fig. 4a, b and c, using different numbers of classes and applying different constraints to χ. The graphs in Fig. 4a shows that when χ was constrained to between 0.4 and 1.0, unacceptable results were obtained having a root mean square error (RMSE) of $\sim$1.15. The correlations for 5, 10, 15 and 25 classes are shown from left to right. Better results were obtained when χ was fixed to the measured mean value of 0.8, as shown in Fig. 4b. However, even better results were achieved (Fig. 4c) when χ varied within a small neighbourhood of the measured mean values between 0.7 and 0.9, which would seem to underline the importance of parameter χ in the inversion process. Free variations of χ lead to situations of instability in the inversion process with unpredictable results; however, small variations around the expected value allowed better accuracy in the retrieval of the remaining parameters.

Regarding the number of classes, the worst result in the three series was obtained when the number of classes was set at 5. When 10, 15, 20 or 25 classes were used, results were essentially the same, therefore a total of 10 classes were selected for the rest of the study (as in Berjón 2007). In this case, the R^2 value obtained was 0.83 and RMSE reached a value of 0.63 for the LAI correlation. Figure 5, (equal to Fig. 4a), shows the standard deviation of retrieved LAI when using 16 repetitions in the inversion procedure for each plot while varying the initial estimates. Average standard deviation was below 0.2, except for plot 12 which was analysed on 17 May 2003, and where the standard deviation reached values as high as 4. In the inversion of data from this plot, one of the 16 repetitions yielded a value of $\sim$20 for LAI in the three control points. Upon elimination of this repetition, the standard deviation became 0.5.

Having obtained these results, the same inversion methodology was then applied separately to barley and wheat plots. Inversion results for barley (Fig. 6a) and wheat plots (Fig. 6b) were obtained constraining χ to 0.7 and 0.9, respectively. Coefficients of

Table 4 Values used to initialize multi-start downhill simplex minimization algorithm used in this study

C_{a+b}	ρ_{soil}	χ	x_1
30	0.4	0.7	0.1
40	0.6	0.9	2

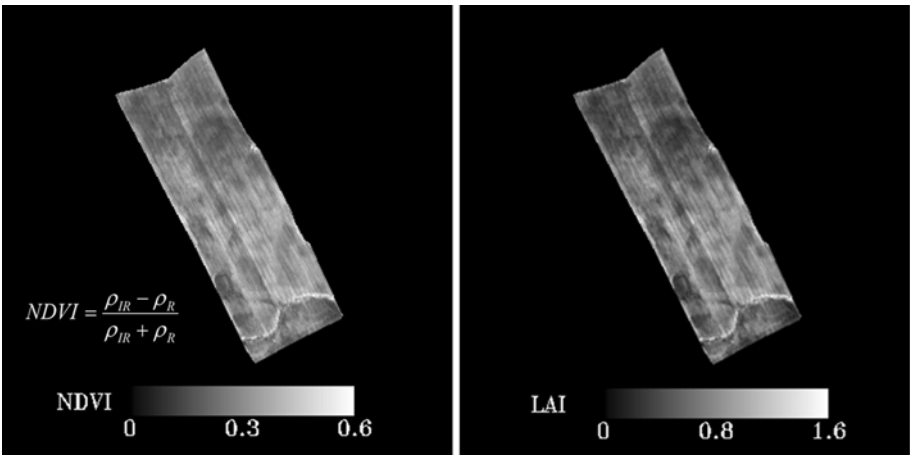

Fig. 3 NDVI (*left*) and LAI (*right*) calculated using NDVI, applying x_1 and x_2 and soil reflectance from the inversion to the exponential relationship

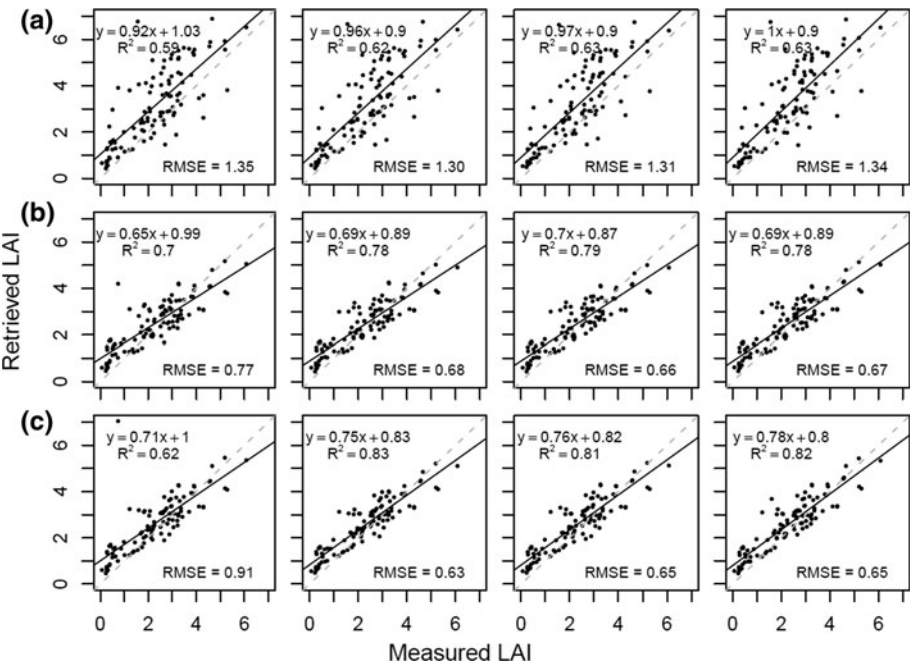

Fig. 4 **a** Comparison between measured LAI and LAI retrieved by inversion, inverting simultaneously x_1(LAI), C_{ab}, soil reflectance and χ ($0.4 < \chi < 1.0$) using 5, 10, 15 and 25 classes (from *left* to *right*). **b** Idem to **a** but with ($\chi = 0.8$). **c** Idem to **a** but χ varying in the interval ($0.7 < \chi < 0.9$)

determination and RMSE were 0.89 and 0.64 for barley and 0.56 and 0.61 for wheat, respectively. Differences in the coefficients of determination were mainly due to the lower range of LAI for the wheat plots compared to barley; a similar RMSE was obtained in both cases. As previously mentioned, chlorophyll content measured over each plot was

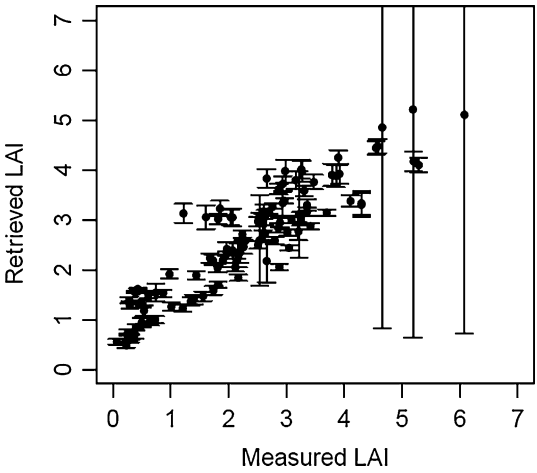

Fig. 5 *Error* (shown as the standard deviation over the retrieved LAI) derived from the differences obtained from the initial estimations

averaged, giving values ranging between 20 and 60 μg/cm^2 for the 16 plots in question. A comparison between chlorophyll content as measured and as estimated by the three inversions is shown in Fig. 7 for each plot for 16 May 2003. Mean C_{a+b} values and standard deviation for each of the three tests were 38 ± 3, 31 ± 3 and 37 ± 3 μg/cm^2, respectively. The RMSE values for the three inversions were 9, 10 and 9.3 μg/cm^2, respectively.

Application of the standard inversion procedure

The standard inversion method uses a single spectrum representing a given spatial point (a pixel or the average of a reduced number of pixels around a given point) and date. The multi-start downhill simplex method, as previously described, was used for iterative optimization.

However, according to the results obtained, the standard inversion method retrieved reasonable values only when one or two parameters (i.e. LAI or LAI and chlorophyll) were to be retrieved and provided that a good estimate of the remaining parameters could be made (taking into account additional information such as vegetation phenology or previous knowledge of the remaining parameters). In the case of this study, simultaneous retrieval of the four parameters yielded inconsistent results when parameters were allowed to vary freely within realistic ranges.

Figure 8a and b show the results obtained using the standard inversion method across the 50 control points, using the images from 6 April and 17 May 2003, respectively, retrieving LAI and ρ_{soil}. The remaining parameters were fixed as follows: $\chi = 0.8$, $C_{ab} = 32$ μg/cm^2 for barley and $C_{ab} = 34$ μg/cm^2 for wheat. As can be seen, the result of this inversion yielded an acceptable correlation for the image from 6 April, with a $R^2 = 0.75$ and a RMSE = 0.94, but not for that of 17 May, which shows a poor correlation with $R^2 = 0.28$ and RMSE = 1. Upon combining the information from the two images, the results of the inversion were improved as shown in Fig. 8c where $R^2 = 0.55$ and RMSE = 0.97. However, it should be emphasized that although the values of LAI retrieved by inversion were acceptable compared to measured values, retrieved values for ρ_{soil} differed from expected values and over 95 % were between 1 and 3, rather than between 0 and 1. The latter inversion (Fig. 8c) was relatively simple (i.e. only two

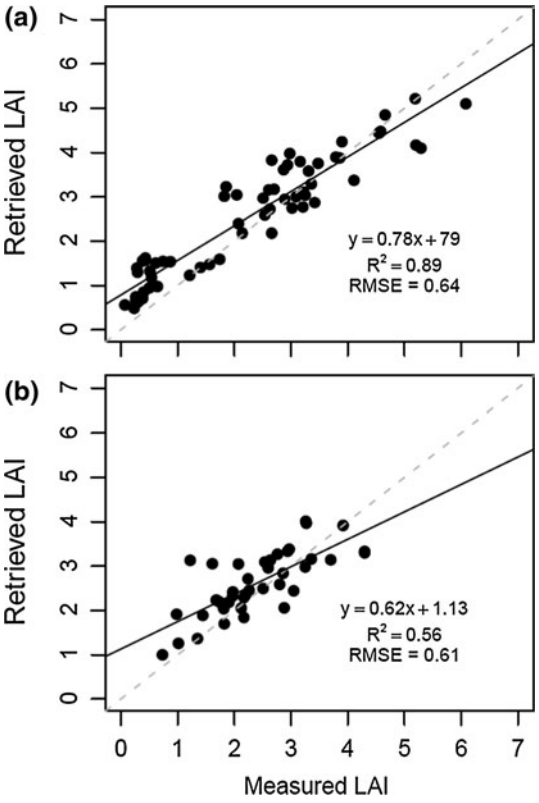

Fig. 6 Comparison between measured LAI and LAI retrieved by inversion using 10 classes, **a** considering only barley plots and **b** considering only wheat plots

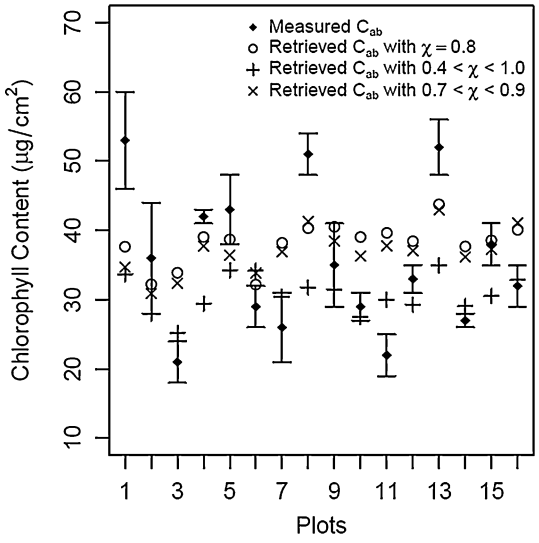

Fig. 7 Comparison between measured and estimated chlorophyll content for each plot

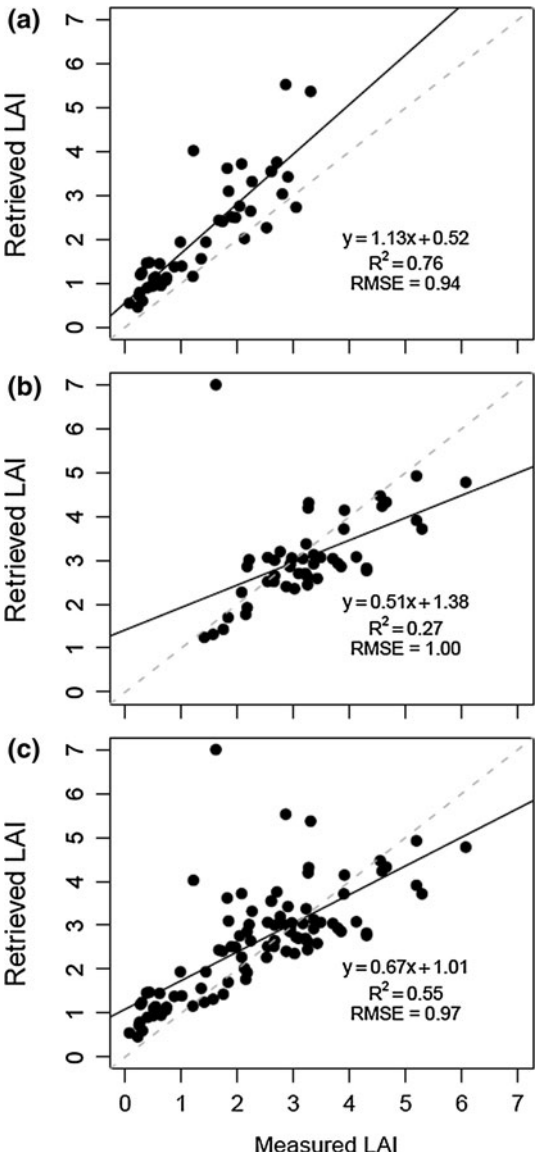

Fig. 8 Comparison between the measured LAI and the LAI retrieved by the standard inversion procedure over the 50 points, **a** for the image of 6 April 2003, **b** for the image of 17 May and **c** for both images

retrieved parameters) and might be comparable to the results shown in Fig. 4b (where $\chi = 0.8$). As shown, the correlations for the LAI parameter were poorer in the standard inversion than in the approach described in this study.

Conclusions

A model inversion method for biophysical parameter retrieval was proposed. The method was then implemented to estimate LAI using remote sensing data constrained by a vegetation index. The proposed approach was tested on homogeneous crop canopies, i.e. wheat

and barley, using high spatial resolution satellite imagery and ground-measured LAI for validation. The method was shown to drastically reduce the amount of a priori knowledge needed to estimate LAI. The inclusion of the spatial data for each plot yielded better results than the standard model-inversion methods based on single spectra. Application of the inversion procedure to high spatial resolution images from the QuickBird 2 satellite for barley and wheat LAI estimation yielded $R^2 = 0.89$ (RMSE = 0.64) and $R^2 = 0.56$ (RMSE = 0.61), respectively. The results show that this inversion method performs efficiently without the need for initial estimates in the multi-start iterative optimization, thus eliminating the need for a large number of restarts.

Acknowledgments The author gratefully acknowledges the extensive help provided by Dr. Richard Santer (Maison de la Recherche en Environnement Naturel, Université Cote d'Opale, France) on atmospheric correction. Financial support was provided by project GR-220 of the Government of the Autonomous Community of "Junta de Castilla y León" and now by projects AGL2009-13105, CGL2011-23413 of the Spanish "Ministerio de Educación y Ciencia". Thanks to AERONET and PHOTON teams for provided atmospheric parameters, and also to Department of Agricultural Engineering of E. T. S. of Agriculture Engineering of Palencia at the University of Valladolid for their help.

References

Allen, W. A., Gausman, H. W., Richardson, A. J., & Thomas, J. R. (1969). Interaction of isotropic light with a compact leaf. *Journal of the Optical Society of America, 59*, 1376–1379.

Allen, W. A., Gayle, T. V., & Richardson, A. J. (1970). Plant-canopy irradiance specified by the Duntley equations. *Journal of the Optical Society of America, 60*, 372–376.

Aparicio, N., Villegas, D., Casadesus, J., Araus, J., & Royo, C. (2000). Spectral vegetation indices as nondestructive tools for determining durum wheat yield. *Agronomy Journal, 92*, 83–91.

Atzberger, C. (2004). Object-based retrieval of biophysical canopy variables using artificial neural nets and radiative transfer models. *Remote Sensing of Environment, 93*, 53–67.

Bacour, C., Jacquemoud, S., Leroy, M., Hautecoeur, O., Weiss, M., Prévot, L., et al. (2002). Reliability of the estimation of vegetation characteristics by inversion of three canopy reflectance models on airborne POLDER data. *Agronomie, 22*, 555–565.

Bennouna, Y. S., Cachorro, V. E., Torres, B., Toledano, C., Berjón, A., De Frutos, A. M., et al. (2013). Atmospheric turbidity determined by the annual cycle of the aerosol optical depth over north-center Spain from ground (AERONET) and satellite (MODIS). *Atmospheric Environment, 67*, 352–364.

Berjón, A. (2007). *Determinación de parámetros biofísicos de la cubierta vegetal mediante inversión de modelos de transferencia radiativa*. Ph.D. thesis, University of Valladolid.

Berjón, A. J., Cachorro, V. E., Zarco-Tejada, P. J., Frutos, A. M., & Toledano, C. (2006). Vegetation spectral reflectance inversion considering the temporal variation of biophysical parameters. In J. A. Sobrino (Ed.), *Second recent advances in quantitative remote sensing* (pp. 620–625). Valencia: Universitat de València.

Bunnik, N. J. J. (1978). Spectral reflectance and transmittance of single leaves. In H. Veenman & B. U. Zonen (Eds.), *The multispectral reflectance of shortwave radiation by agricultural crops in relation with their morphological and optical properties* (pp. 10–22). Veenman: Wageningen.

Cachorro, V. E., Berjón, A., Vergaz, R., & De Frutos, A. M. (2001). Creación de una base de datos espectroradiometricos de la reflectancia de cultivos de secano. In J. I. Rosell & J. A. Martinez-Casasnovas (Eds.), *Teledetección, Medio Ambiente y Cambio Global. Proceedings of the IX Congreso Nacional de Teledetección* (pp. 41–44). Lleida: Universitat de Lleida.

Cachorro, V. E., Duran, P., De Frutos, A. M., Vergaz, R., & Hernández, S. (1997). Modelización de la transferencia radiativa en la atmósfera. Comparación con datos experimentales a nivel de suelo y determinación de la reflectancia de la atmósfera. In C. Hernandez & J. E. Arias (Eds.), *Teledetección Aplicada a la Géstion de Recursos Naturales y Medio Litoral Marino* (pp. 42–45). Santiago de Compostela: Asociación Española de Teledetección.

Cachorro, V. E., Vergaz, R., & De Frutos, A. M. (2000). A model for atmospheric correction of DAIS hyperspectral imager sensor based on experimental measurements. In J. L. Casanova (Ed.), *Remote sensing in the 21st century: Economic and environmental applications* (pp. 541–548). Rotterdam: Balkema.

Campbell, G. S. (1986). Extinction coefficients for radiation in plant canopies calculated using an ellipsoidal inclination angle distribution. *Agricultural and Forest Meteorology, 36*, 317–321.
Campbell, G. S. (1990). Derivation of an angle density function for canopies with ellipsoidal leaf angle distributions. *Agricultural and Forest Meteorology, 49*, 173–176.
Carlson, T. N., & Ripley, D. A. (1990). On the relation between NDVI, fractional vegetation cover, and leaf area index. *Remote Sensing of Environment, 62*, 241–252.
Combal, B., Baret, F., Weiss, M., Trubuil, A., Macé, D., Pragnère, A., et al. (2002). Retrieval of canopy biophysical variables from bidirectional reflectance using prior information to solve the ill-posed inverse problem. *Remote Sensing of Environment, 84*, 1–15.
Darvishzadeh, R., Skidmore, A., Schlerf, M., & Atzberger, C. (2008). Inversion of radiative transfer model for estimating LAI and chlorophyll in a heterogeneous grassland. *Remote Sensing of Environment, 112*, 2592–2604.
Feret, J.-B., François, C., Asner, G. P., Gitelson, A. A., Martin, R. R., Bidel, I. P. R., et al. (2008). PROSPECT-4 and 5: Advances in the leaf optical properties model separating photosynthetic pigments. *Remote Sensing of Environment, 112*, 3030–3043.
Fernández, N., Paruelo, J., & Delibes, M. (2010). Ecosystem functioning in protected and altered Mediterranean environments: A remote sensing classification in Doñana, Spain. *Remote Sensing of Environment, 114*, 211–220.
Gausman, H. W., Allen, W. A., Cardenas, R., & Richardson, A. J. (1970). Relation of light reflectance to histological and physical evaluation of cotton leaf maturity. *Applied Optics, 9*, 545–552.
Goel, N. S. (1988). Models of vegetation canopy reflectance and their use in estimation of biophysical parameters from reflectance data. *Remote Sensing Reviews, 4*, 1–222.
Goel, N. S., & Strebel, D. E. (1983). Inversion of vegetation canopy reflectance models for estimating agronomic variables. I. Problem definition and initial results using the Suits model. *Remote Sensing of Environment, 13*, 487–507.
Green, E. P., Mumby, P. J., Edwards, A. J., & Clark, C. D. (2000). *Remote sensing handbook for tropical coastal management*. Paris: UNESCO.
Gueymard, C. (2004). The sun's total and spectral irradiance for solar energy applications and solar radiation models. *Solar Energy, 76*, 423–453.
Gutman, G. G. (1991). Vegetation indices from AVHRR: An update and future prospects. *Remote Sensing of Environment, 35*, 121–136.
Haboudane, D., Miller, J. R., Tremblay, R., Zarco-Tejada, P. J., & Dextraze, L. (2002). Integrated narrowband vegetation indices for predicting chlorophyll content for application to precision agriculture. *Remote Sensing of Environment, 81*, 416–426.
Houborg, R., Soegaard, H., & Boegh, E. (2007). Combining vegetation index and model inversion methods for the extraction of key vegetation biophysical parameters using Terra and Aqua MODIS reflectance data. *Remote Sensing of Environment, 106*, 39–58.
Jacquemoud, S., & Baret, F. (1990). PROSPECT: A model of leaf optical properties spectra. *Remote Sensing of Environment, 34*, 75–91.
Jacquemoud, S., Baret, F., Andrieu, B., Danson, F. M., & Jaggard, K. (1995). Extraction of vegetation biophysical parameters by inversion of the PROSPECT + SAIL models on sugar beet canopy reflectance data. Application to TM and AVIRIS sensors. *Remote Sensing of Environment, 52*, 163–172.
Jacquemoud, S., Verhoef, W., Baret, F., Bacour, C., Zarco-Tejada, P. J., Asner, G. P., et al. (2009). PROSPECT + SAIL models: A review of use for vegetation characterization. *Remote Sensing of Environment, 113*, S56–S66.
Kaufman, Y. J., Tanré, D., & Boucher, O. (2002). A satellite view of aerosols in the climate system. *Nature, 419*, 215–223.
King, M. D., Kaufman, Y. J., Tanré, D., & Nakajima, T. (1999). Remote sensing of atmospheric aerosols from space: Past, present and future. *Bulletin of the American Meteorological Society, 80*, 2229–2259.
Kuusk, A. (1985). The hot spot effect of a uniform vegetative cover. *Soviet Journal of Remote Sensing, 3*, 645–658.
Kuusk, A. (1995). A Markov chain model of canopy reflectance. *Agricultural and Forest Meteorology, 76*, 221–236.
Lauvernet, C., Baret, F., Hascoët, L., Buis, S., & Le Dimet, F.-X. (2008). Multitemporal patch ensemble inversion of couplet surface-atmosphere radiative transfer for and surface characterization. *Remote Sensing of Environment, 112*, 851–862.
Liang, S. (2004). *Quantitative remote sensing of land surfaces*. Hoboken: Wiley.
Liang, S. (2008). *Advances in land remote sensing: System, modelling, inversion and application*. New York: Springer.

Liedtke, J. (2002). QuickBird-2 System Description and product overview. JACIE Workshop. Washington, DC. http://calval.cr.usgs.gov/wordpress/wp-content/uploads/16Liedtk.pdf. Accessed 16 April 2013.

Lu, L., Li, X., Ma, M., Che, G., Huang, T., Bogaert, C. L., et al. (2004). Investigating relationship between Landsat ETM + data and LAI in a semi-arid grassland of Northwest China. In *IGARSS 2004—2004 IEEE International Geoscience and Remote Sensing Symposium Proceedings* (pp. 3622–3625). Piscataway: IEEE.

Migdall, S., Bach, H., Bobert, J., Wehrhan, M., & Mauser, W. (2009). Inversion of a canopy reflectance model using hyperspectral imagery for monitoring wheat growth and estimating yield. *Precision Agriculture, 10*, 508–524.

Morisette, J. T., Baret, F., Privette, J. L., Myneni, R. B., Nickeson, J. E., Garrigues, S., et al. (2006). Validation of global moderate-resolution LAI products: A framework proposed within the CEOS land product validation subgroup. *IEEE Transactions on Geoscience and Remote Sensing, 44*, 1804–1817.

Nelder, J. A., & Mead, R. (1965). A simplex method for function minimization. *Computer Journal, 7*, 308–313.

Richardson, A. J., Wiegand, C. L., Wanjura, D. F., Dusek, D., & Steiner, J. L. (1992). Multisite analyses of spectral-biophysical data for sorghum. *Remote Sensing of Environment, 41*, 71–82.

Saltelli, A. (2002). Sensitivity analysis for importance assessment. *Risk Analysis, 22*, 579–590.

Saltelli, A., Tarantola, S., & Chan, K. P. S. (1999). A quantitative model-independent method for global sensitivity analysis of model output. *Technometrics, 41*, 39–56.

Steven, M. D., Malthus, T. J., Baret, F., Xu, H., & Chopping, M. J. (2003). Intercalibration of vegetation indices from different sensor systems. *Remote Sensing of Environment, 88*, 412–422.

Suits, G. H. (1972). The calculation of the directional reflectance of a vegetative canopy. *Remote Sensing of Environment, 2*, 117–125.

Turner, D. P., Cohen, W. B., Kennedy, R. E., Fassnacht, K. S., & Briggs, J. M. (1999). Relationships between leaf area index and Landsat TM spectral vegetation indices across three temperate zone sites. *Remote Sensing of Environment, 70*, 52–68.

Verhoef, W. (1984). Light scattering by leaf layers with application to canopy reflectance modelling: The SAIL model. *Remote Sensing of Environment, 16*, 25–141.

Verhoef, W., & Bach, H. (2007). Coupled soil-leaf-canopy and atmosphere radiative transfer modelling to simulate hyperspectral multi-angular surface reflectance and TOA radiance data. *Remote Sensing of Environment, 109*, 166–182.

Vermote, E. F., Tanré, D., Deuzé, J. L., Herman, M., & Mocrette, J. J. (1997). Second simulation of the satellite signal in the solar spectrum, 6S: An overview. *IEEE Transactions on Geoscience and Remote Sensing, 35*, 675–686.

Vile, D., Garnier, E., Shipley, B., Laurent, G., Navas, M. L., Roumet, C., et al. (2005). Specific leaf area and dry matter content estimate thickness in laminar leaves. *Annals of Botany, 96*, 1129–1136.

Wang, Y. P., & Jarvis, P. G. (1988). Mean leaf angles for the ellipsoidal inclination angle distribution. *Agricultural and Forest Meteorology, 43*, 319–321.

Wellburn, A. R. (1994). The spectral determination of chlorophylls *a* and *b*, as well as total carotenoids using various solvents with spectrophotometers of different resolutions. *Journal of Plant Physiology, 144*, 307–313.

Zarco-Tejada, P. J., Berjón, A. J., Lopez, R., Miller, J. R., Martin, P., Cachorro, V. E., et al. (2005). Assessing vineyard condition with hyperspectral indices: Leaf and canopy reflectance simulation in a row structured discontinuous canopy. *Remote Sensing of Environment, 99*, 271–287.

Zarco-Tejada, P. J., Miller, J. R., Morales, A., Berjón, A., & Agüera, J. (2004). Hyperspectral indices and model simulation for chlorophyll estimation in open-canopy tree crops. *Remote Sensing of Environment, 90*, 463–476.

Zarco-Tejada, P. J., Miller, J. R., Noland, T. L., Mohammed, G. H., & Sampson, P. H. (2001). Scaling-up and model inversion methods with narrowband optical indices for chlorophyll content estimation in closed forest canopies with hyperspectral data. *IEEE Transactions on Geoscience and Remote Sensing, 39*, 1491–1507.

Zhangshi, Y., & Williams, T. H. L. (1997). Obtaining spatial and temporal vegetation data from Landsat MSS and AVHRR/NOAA satellite images for a hydrological model. *Photogrammetric Engineering and Remote Sensing, 63*, 69–77.